Reprinted from MONTHLY WEATHER REVIEW, Vol. 116, No. 2, February 1988
American Meteorological Society

Three-Dimensional Air Motions over the Baiu Front Observed by a VHF-Band Doppler Radar: A Case Study

SHOICHIRO FUKAO

Radio Atmospheric Science Center, Kyoto University, Uji, Kyoto, Japan

MANABU D. YAMANAKA

Faculty of Education, Yamaguchi University, Yoshida, Yamaguchi, Japan

TORU SATO, TOSHITAKA TSUDA AND SUSUMU KATO

Radio Atmospheric Science Center, Kyoto University, Uji, Kyoto, Japan

(Manuscript received 4 October 1986, in final form 16 March 1987)

ABSTRACT

Upper-tropospheric three dimensional air motions have been observed for the first time during the Baiu period in 1984 by using a 46.5 MHz Doppler radar in Japan. This radar, called the MU radar, operates with an antenna aperture of 8330 m^2 and peak and average radiation powers of 1000 and 50 kW, respectively. It can steer the antenna beam up to 30° from the zenith in each interpulse period. With the aid of this fast beam steerability the MU radar can measure the three dimensional air motion. Resolutions in time and altitude of the present observations are 100 s and 150 m, respectively. Referring to the routine rawinsonde observations the following results are obtained on the air motion over the Baiu front: 1) the observed mean meridional motion is upward and northward as expected but deviates upward from the frontal surface and pseudo-isentropes; 2) the upper-tropospheric mesoscale wind variations are not strongly correlated with the lower-tropospheric frontal activity such as precipitation; and 3) intense updrafts of 0.5–1 m s^{-1} appear at an interval of approximately 22 h. This interval suggests that the updrafts are caused by neutral symmetric motion.

1. Introduction

Mesosphere–stratosphere–troposphere (MST) radars are sensitive VHF/UHF Doppler radars. This type of radar is a powerful tool for the study of air motions because the echoes return from the atmospheric (refractive index) fluctuations (e.g., Green et al., 1979; Harper and Gordon, 1980; Balsley and Gage, 1980, 1982; Larsen and Röttger, 1982; Gage and Balsley, 1984; Röttger, 1984, for reviews). Resolutions in height and time obtained by this technique are far better than those of other conventional meteorological instruments such as rawinsondes and rocketsondes. Application of this technique to the study of mesoscale meteorological phenomena has been made in Western Europe (Röttger, 1979; Röttger and Schmidt, 1981; Ecklund et al., 1985) and in the east of the Rocky Mountains (Ecklund et al., 1982). The MST radar technique is expected to open a new era of the radar meteorology in the near future.

This paper is concerned principally with the first MST radar observation of dynamical aspects of the Baiu frontal atmosphere. The MST radar employed for the present observation is the middle and upper atmosphere radar (the MU radar) at Shigaraki, Japan (34.85°N, 136.10°E; see Fig. 1 for its location). This radar is a new generation MST radar which employs an active phased-array system (Fukao et al., 1985a,b). Fukao et al. (1985d) used this system for the first time for tropospheric observations of a precipitating atmosphere, and recently detected precipitation motions simultaneously with the ambient air motion (Fukao et al., 1985c). The air and precipitation motions together with radar reflectivity associated with a cold-frontal passage were measured with the same radar by Wakasugi et al. (1985). This radar system has also been used to determine the raindrop size distribution without any assumption on vertical air motion (Wakasugi et al., 1986).

The Baiu front is known as the most activated subtropical front (Ninomiya, 1984), which appears over China and Japan during June and July and accompanies severe subsynoptic-scale rainfalls (see Yoshino, 1977 for a climatical survey of the Baiu front). The activation is not caused only by the synoptic-scale baroclinic conditions (e.g., Tokioka, 1973). The observational studies conducted so far related to the Baiu

Corresponding author address: Dr. Fukao, Radio Atmospheric Science Center, Kyoto University, Uji, Kyoto 611, Japan

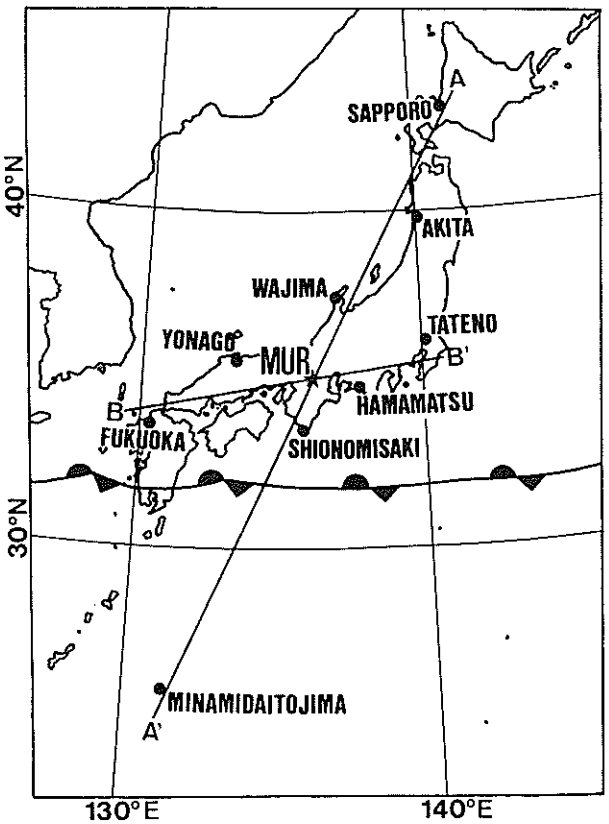

FIG. 1. Location of the MU radar (MUR) and the rawinsonde stations used in the cross section analysis (Fig. 4). Sapporo (SA; 47412), Akita (AK; 47582), Wajima (WA; 47600), Shionomisaki (SH; 47778), and Minamidaitojima (MI; 47945) are lined approximately along the baseline *AA'*, while Fukuoka (FU; 47807), Yonago (YO; 47744), Shionomisaki, Hamamatsu (HA; 47681), and Tateno (TA; 47646) are near the baseline *BB'*. The Baiu frontal position is transcribed from the surface chart at 2100 LST 28 June 1984 (JMA, 1984a).

frontal atmosphere are classified into the following three categories: 1) synoptic and climatical analyses based on routine ground-based and rawinsonde observations (e.g., Murakami, 1951; Matsumoto et al., 1970; Ninomiya and Akiyama, 1971; Yoshizumi, 1978; Akiyama, 1979; Ninomiya, 1983, 1984); 2) visible and infrared imageries by meteorological satellites (e.g., Ninomiya et al., 1981; Akiyama, 1984); and 3) radar and AMeDAS (*A*utomated *Me*teorological *D*ata *A*cquisition *S*ystem) observations of precipitation (e.g., Ninomiya and Akiyama, 1972; Akiyama, 1978; 1979). The first category is concerned with dynamical phenomena such as low-level jets (~500 hPa) and frontal cyclones. The second and third categories principally discuss cloud-physical rather than dynamical aspects. Therefore, as for the subsynoptic-scale dynamics of the Baiu frontal atmosphere, only little knowledge has been obtained so far. The dynamical aspects are considered to be a key to the "missing link" for elucidation of the Baiu front activation.

In this paper we report some observations that are considered to be typical of the Baiu frontal atmosphere. The observed variations of wind field and echo intensity are compared with routine observations of the Japan Meteorological Agency (JMA). Both detailed physical interpretation of the observed results and discussion on their relationship to the Baiu front activation are beyond the scope of the present paper. Despite this, the paper will reveal the potential capability of the MST radar technique for Baiu and other mesometeorological studies, noting that no high-resolution continuous data of the three-dimensional wind field was obtained in the Baiu frontal atmosphere until the present MU radar observation was made in June 1984.

2. MU radar system

The MU radar is a 46.5-MHz Doppler radar using an active phased array system (Fukao et al., 1980). It is composed of 475 Yagi antennas and an equivalent number of solid-state power amplifiers [transmitter-receiver (TR) modules] (Fukao et al., 1985a,b). Each Yagi antenna is driven by a TR module with peak output power of 2.4 kW. All Yagi antennas and TR modules are grouped into 25 subarrays (i.e., 19 Yagi antennas and TR modules constitute one subarray). The nominal peak and average radiation powers of the whole system are 1000 and 50 kW, respectively. This system makes it possible to steer the antenna beam up to 30° from the zenith in each interpulse period. The basic parameters of the MU radar are shown in Table 1. Further details of the system have been given by Kato et al. (1984) and Fukao et al. (1985a,b).

The MU radar-deduced winds have been often compared with the results of other well-established

TABLE 1. Basic parameters of the MU radar.

Radar system:	Monostatic pulse radar; active phased array system
Operational frequency:	46.5 MHz
Antenna:	Circular array of 475 crossed Yagi antennas
Aperture:	8,330 m² (103 m in diameter)
Beam width:	3.6° (half power for full array)
Steerability:	Steering is completed in each IPP.
Beam directions:	1657; 0–30° off-zenith angle
Transmitter:	475 solid-state amplifiers (TR-modules; each wtih output power of 2.4 kW peak and 120 W average)
Peak power:	1000 kW (max)
Average power:	50 kW (duty ratio 5%) (max)
Bandwidth:	1.65 MHz (max) (pulse width: 1–512 μs variable)
IPP:	400 μs–65 ms (variable)
Receiver:	
Dynamic range:	70 dB
A/D converter:	12 bits × 8 channels
Pulse compression:	Binary phase-coding up to 32 elements (Barker and complementary codes presently in use)

meteorological techniques of wind measurement. In the troposphere and the lower stratosphere the radar-deduced winds are favorably compared with the results of rawinsonde balloons, while they are consistent with the results of rocketsonde observations in the mesosphere (Fukao et al., 1985b; Tsuda et al., 1985; Kato et al., 1986).

Since the present observation was conducted before the full system of the MU radar was completed in November 1984 (Kato et al., 1986), the full capabilities were only partially employed. A nominal beam width of 4.0° and peak transmitted power of 760 kW were selected.

3. VAD observation

The MU radar has a Doppler capability which enables radial velocity measurements along the radar beam direction. For the present observation a velocity–azimuth–display (VAD) technique, which was first applied to the VHF MU radar by Wakasugi et al. (1985), was employed. The antenna beam was sequentially steered to 16 oblique directions in different azimuths keeping a zenith angle of 15°. The beam direction was switched every interpulse period (400 μs). Thus, one scan on a VAD circle is completed in 6.4 m s. The diameter of the VAD circle is approximately 2.7 and 5.4 km at altitudes of 5 and 10 km, respectively, which is quite smaller than that for conventional (microwave) meteorological Doppler radar observations. With this technique the three dimensional air motion with a horizontal scale larger than this distance is detectable (see Fukao et al., 1986 for details).

The transmitted pulse was phased-modulated by a 16-element complementary code with 1 μs baud length, corresponding to a height (or range) resolution of 150 m. The echo from each beam was sampled at 64 heights in an altitude range of 5.21–14.3 km at 150 m intervals. After coherently integrating over 8 circle scan periods (51.2 m s), Doppler velocity spectra were estimated every 6.5 s in real time from 128 point complex fast Fourier transforms and then averaged for approximately 100 s. Thus, a vertical profile of VAD wind is obtained about every 100 s in the present case, quite faster than by microwave meteorological Doppler radars.

The radial velocity resolution is approximately 10 cm s^{-1}, and the expected accuracy of a 1-h averaged wind velocity is of the order of 1 cm s^{-1}. Since we used a 16 element complementary code (total pulse length of 16 μs) for pulse compression, the present observation was limited to above an altitude of about 5.21 km.

The present observation was conducted over a two-day period on 28–30 June 1984. Figure 2 shows plots of radial velocity as function of azimuth (VAD) obtained in approximately a 100 s interval at 5.21–10.0 km. It is noted that the VAD plots always yield nearly sinusoidal variations as shown in this diagram, suggesting that the predominant horizontal scale of wind variations is, in general, larger than the VAD circles or a few kilometers. The horizontal motion is derived from the first harmonic by a least squares fitting harmonic analysis, while the vertical motion is derived from the zeroth harmonic. Although slight fluctuations of wind (less than a few m s^{-1}) with scales less than the VAD circles are observed to exist in Fig. 2, the velocity estimates seem to represent the real three-dimensional wind over the MU radar with an accuracy and reliability sufficient for meteorological application.

4. Synoptic-scale meteorological features

As will be discussed in subsection 6b, the present observation is made from a fixed ground station and, in general, the spatial scale cannot be specified from the observed temporal variation. However, in the following the temporal variations with time scales larger than one day are called "synoptic-scale," while those with scales less than one day are called "mesoscale" for convenience. In this section, some general features of the synoptic-scale atmospheric structure which was observed during the observational period are discussed.

Figure 3 shows the time–latitude cross sections of the surface pressure and the cloud distribution along the 136°E meridian during the entire observational period. The surface pressure chart is transcribed from the JMA 12-h interval weather chart (JMA, 1984a), while the cloud distribution chart is depicted in reference to the Geostationary Meteorological Satellite (GMS) cloud nephanalyses (JMA, 1984b). As observed in the surface pressure chart the Baiu front stayed in

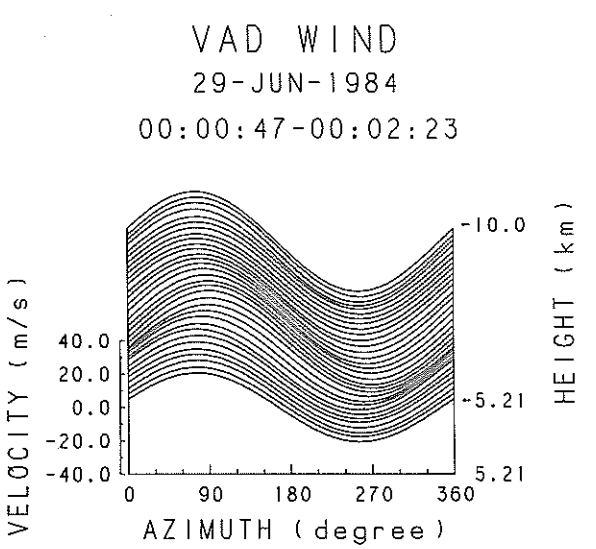

FIG. 2. Velocity–azimuth–display (VAD) plots of radial velocity against azimuth angle observed at 5.21–10.0 km in an approximately 100 s interval around 0000 LST 29 June 1984. Keeping the zenith angle at 15°, the antenna beam is steered every IPP (400 μs) in 16 directions with azimuth angles of 0° (north), 20°, 45°, 65°, 90° (east), 110°, 135°, 155°, 180° (south), 200°, 225°, 245°, 270° (west), 290°, 315° and 335°. The velocity scale applies only to the lowest VAD plot.

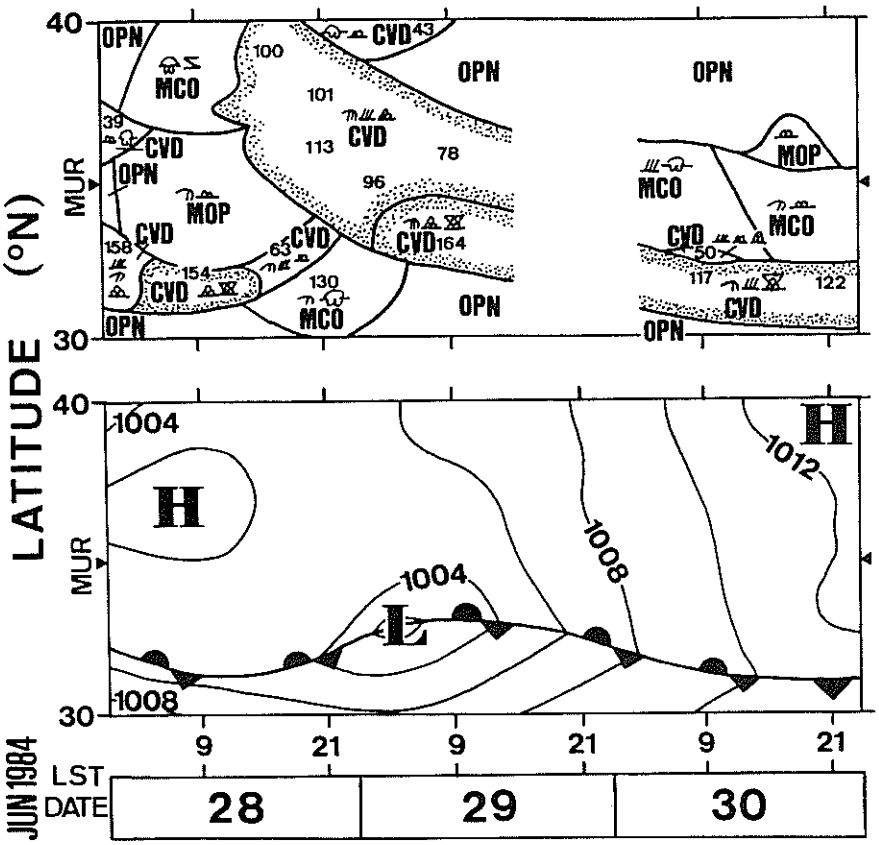

FIG. 3. Time–latitude cross sections of cloud distribution (upper diagram) and surface pressure (lower diagram). The cloud distribution diagram is transcribed based on the nephanalysis of cloud observations made by GMS (JMA, 1984b). The cloud amount is indicated by "OPN" (<20%), "MOP" (20–50%), "MCO" (50–80%), and "CVD" (>80%) with stipplings for systematically extending thick cloud systems and active convective clouds. Cloud-top heights are indicated in units of 100 m. GMS data were not available at 2100 LST 29 June. The surface pressure chart is depicted based on the weather maps (JMA, 1984a).

the south of Japan throughout the observational period. A remarkable cloud system with a considerably high cloud top (~11 km) covered the radar site from approximately 1600 LST 28 June 1984. It is observed in these diagrams that mesoscale cyclogenesis is related to the development of the cloud system as well as a northward displacement of the Baiu front. The cyclone center passed the 136°E meridian at 0300 LST.

Vertical cross sections of equivalent potential temperature and horizontal wind at 2100 LST (1200 UTC) 28 June 1984 are shown in Fig. 4. They are produced from the routine rawinsonde data (JMA, 1984c) obtained along two baselines *AA'* and *BB'* indicated in Fig. 1. All rawinsonde stations are operated by JMA except the Hamamatsu station which is operated by the Japan Defense Agency. The two cross sections give approximately latitude–altitude and longitude–altitude cross sections that are nearly perpendicular and parallel to the Baiu front, respectively. In both diagrams geometric altitude is used by transforming from geopotential height with the aid of the free-air gravity correction in both the vertical and meridional directions.

Figure 4 illustrates some features well known to be typical of subtropical fronts (see Ninomiya, 1984, and references therein). The Baiu front was located at 2–4 km altitude (~800–650 hPa level) over the MU radar, and reached up to a tropopause folding. The tropopause was located around 16 km in altitude (~110 hPa level) over the radar site. The pseudo-isentropes in this diagram clearly show strongly stable stratification in the stratosphere, and unstable stratification in the lower troposphere. They also indicate stratosphere–troposphere air exchange along the frontal surface. The subtropical jet stream existed between the tropopause and the front at approximately 41°N, and the lower-level jet was observed around 5 km in altitude over the radar site. It is noted that some day-to-day variations and multi-layered structures were observed, particularly near the tropopause folding (cf., Shapiro, 1980).

The *BB'* section in Fig. 4 shows a zonal wavelike

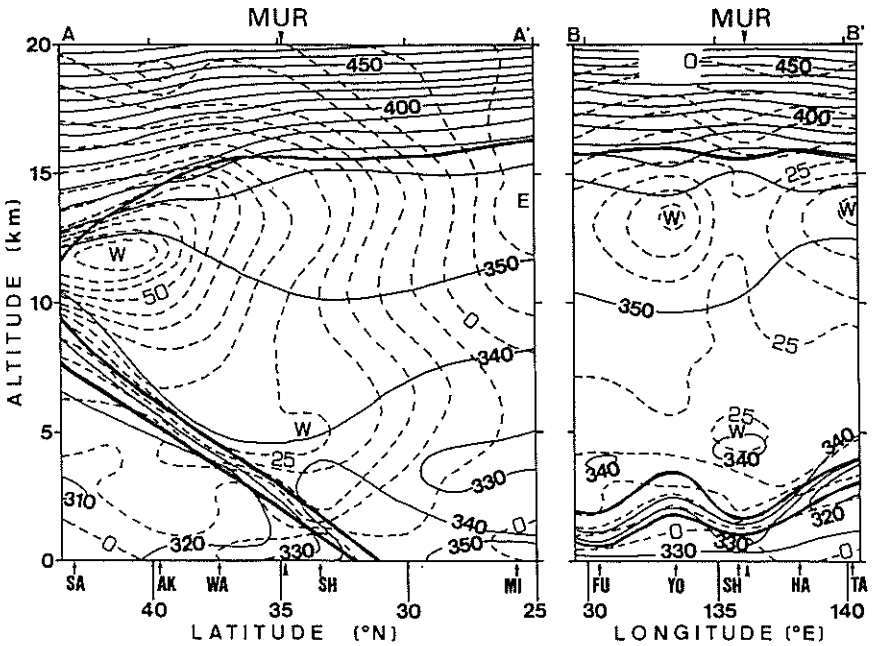

FIG. 4. Vertical cross sections of equivalent potential temperature (K; solid lines) and zonal wind velocity (m s^{-1}; broken lines) at 2100 LST on 28 June 1984 along the baseline *AA'* (left) and *BB'* (right) indicated in Fig. 1. Thick solid lines above and below 10 km show the tropopause and the frontal surface, respectively. Both are produced based on JMA (1984c).

structure with a wavelength of 500–600 km in the whole troposphere. This is probably not a true wave phenomenon but presumably an apparent one as shown in the following. The mesoscale cyclone observed in Fig. 3 has a zonal wavelength of 1000 km or longer, which is typical of the Baiu front associated cyclones. In the surface weather chart corresponding to the time of Fig. 4 (the frontal position is transcribed in Fig. 1) the cyclone center was found near 129°E and a topographical fold was seen near 133°E. However, the latter disappeared entirely in the 850 hPa chart and was not included in Fig. 4. If the cyclone is observed from stations north or south of baseline *BB'* (Fig. 1), an apparent wavelike structure is generated in the longitude–altitude cross section as observed in Fig. 4. Therefore, concerning the synoptic-scale structure of the troposphere near the Baiu front, the meridional variation is considered to dominate the zonal one, that is the field is strongly symmetric with respect to the north pole.

5. Results of radar observations

a. Echo intensity

Figure 5 shows a time–height cross section of the echo intensity caused by atmospheric refractive index fluctuations observed in the northward beam direction. The echo returns are primarily confined to altitudes below 12 km, much lower than the tropopause which is located at approximately 16 km (Fig. 4). In this altitude range the echo power decreases, on average, exponentially with altitude as shown in the right panel of Fig. 5 (Balsley and Gage, 1980). The intense echo power that is persistently observed below 7–8 km is characteristic of tropospheric scattering. However, the echo power varies quite differently during 1800–2200 LST 28 June; the intense echo power disappears during this interval. Similar very weak echo in the same altitude range is also found during 1600–2200 LST 29 June.

During 1500–1700 LST 28 June, two stable echo layers are observed to descend with time at a speed on the order of 1 km h^{-1} in the altitude range of 7–10 km. Since intense echo layers associated with the frontal surface show a strong aspect sensitivity (Wakasugi et al., 1985), a much stronger echo would have been detected by a vertical beam observation. The layer structure disappears at about 1700 LST.

The precipitation echo in the VHF band can, in principle, be distinguished from the clear air echo, since the Doppler power spectra are bifurcated into air and precipitation particle echoes (Fukao et al., 1985c). In the present observation only the spectral component which is considered to be due to clear air echo and free from scattering due to precipitation particles is employed.

The surface rainfall rates as observed by JMA at their facility in Kinose, 6.9 km north of the MU radar

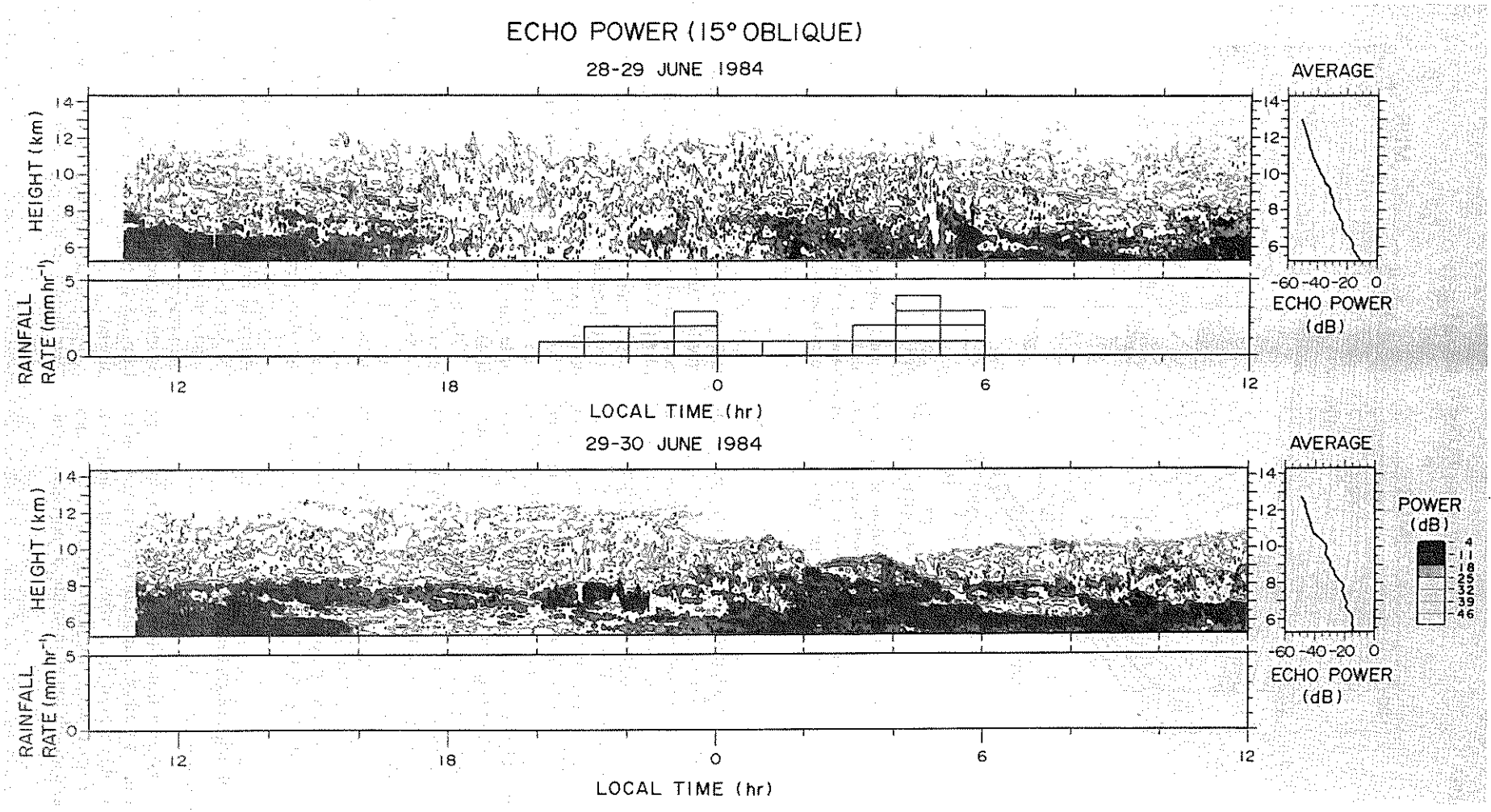

FIG. 5. Time–height cross section of the echo intensity observed in the northward beam direction in a 2-day period 28–30 June 1984. The echo intensity is in an arbitrary unit, and contours are drawn at 7 dB intervals. Unshaded echo regions show the echo intensity of less than −25 dB. The height profiles of echo intensity averaged over the first-half and second-half periods are respectively shown on the right-hand side. Also, the surface rainfall rates as observed by JMA in Kinose are included.

site, are also included in Fig. 5. The period of largest rainfall rate, during 0300–0600 LST 29 June, coincides with that of a relatively intense radar echo. The origin of this enhanced radar echo could be attributed to an increase of reflectivity fluctuations due to the presence of gaseous water vapor (Gossard, 1979; Fukao et al., 1985d).

b. Wind velocity

Figure 6 shows approximately 45 min-averaged vertical profiles of the three velocity components of air motion relative to the mean wind averaged over the whole observational period (~48 h) shown on the right-hand side. The mean horizontal wind is west-southwesterly (east-northeastward), while the upward motion is predominant most of the time. Compared with Fig. 4, it is readily seen that the radar deduced winds are consistent with the rawinsonde winds at the nearest JMA station.

Figure 7 demonstrates time–altitude cross sections of airflow relative to the three-dimensional flow averaged over the first 18-h period. The horizontal relative wind vectors are shown in (a), while the vertical-meridional and vertical-zonal components are illustrated in (b) and (c). The change of the wind vector pattern is as follows: During 1200–1600 LST 28 June a southward or southwestward airflow with a fairly large downward velocity is predominant throughout the height range observed. Then, a relatively strong updraft is observed during 1630–1800 LST. The upward velocity in this period is approximately 1 m s^{-1}. This intense updraft is followed by a northward or northwestward flow with a small downward velocity that predominates in the region observed until 2000 LST. During this period, a westward component persists except below about 7 km where the direction is reversed eastward. Then, a northward or eastward wind predominates until 0000 LST 29 June.

A similar, more long lasting updraft event with a magnitude of about 0.5 m s^{-1} occurs around 1500 LST 29 June, and presumably another event starts just before 1200 LST 30 June (Fig. 6). This feature suggests that the updraft events were breaking out impulsively at an interval of approximately 22 h. However, it is noted that the observed horizontal wind does not have the corresponding periodicity. The echo intensity seems to be recurrently weakened after the updraft event, that suggests a correlation between atmospheric reflectivity and wind velocity fluctuations.

6. Discussions

The high resolution, three dimensional wind velocity data of the present MU radar observation provide new information on the dynamical feature of the Baiu frontal atmosphere. In this section we discuss further the above mentioned results in comparison with the routine meteorological observations. However, more detailed physical interpretations are beyond the scope of the present paper, and a suitable method for analyzing the mesometeorological phenomena based on this new technique is expected to be developed in subsequent studies.

a. Mean meridional circulation over the Baiu front

The average wind velocity shown in the right column of Fig. 6 seems to be consistent with our picture of a subtropical front. Namely, it is composed of a westerly and an upward–northward circulation that roughly parallels the frontal surface. More quantitatively, the mean meridional and vertical velocities at an altitude of 8 km are approximately 6 and 0.15 m s^{-1}, respectively, so that the inclination of the observed meridional circulation is approximately 1/40, while that of the Baiu front is less than 1/100 (Fig. 4). Thus the meridional circulation deviates upward from the frontal surface (and the pseudo-isentropes). This indicates that a considerable amount of air is transported upward by some diabatic, forced motions, such as active convective clouds on the tropical side of the front in the upper troposphere.

This tropospheric air ascent is presumably the counterpart of the stratospheric air descent associated with the tropopause folding, which is one of the most important problems in stratosphere–troposphere coupling studies (see Holton, 1984, for a review). Based on aircraft measurements, Shapiro (1980) has pointed out that a considerable amount of air is transported through turbulent mixing. Similar observations covering a wider range up to the lower stratosphere are desirable to clarify this air transport process.

The aforementioned discussions pertain to the mean field averaged over the whole observational period. As will be discussed in the following, the mean meridional circulation is composed of several small-scale phenomena. In fact, many observational studies by conventional meteorological techniques suggest that Baiu frontal activity cannot be understood only by synoptic-scale phenomena (see references in the third paragraph of section 1). Further, as Hobbs (1978) reviewed, the extratropical cyclone and frontal systems are, in general, organized by mesoscale and microscale phenomena. Therefore, the significance of MU radar observations of the Baiu frontal phenomena as a typical frontal system should be highlighted more, and this point is the principal motivation of the present paper.

b. Frontal activity and upper-tropospheric wind

Since the present observation is made at a fixed ground station, the following three types of mesoscale variations cannot be distinguished from each other:

(i) those developed in time over the MU radar site;
(ii) those due to a spatial variation advected with the mean horizontal velocity u of the synoptic-scale motions; and

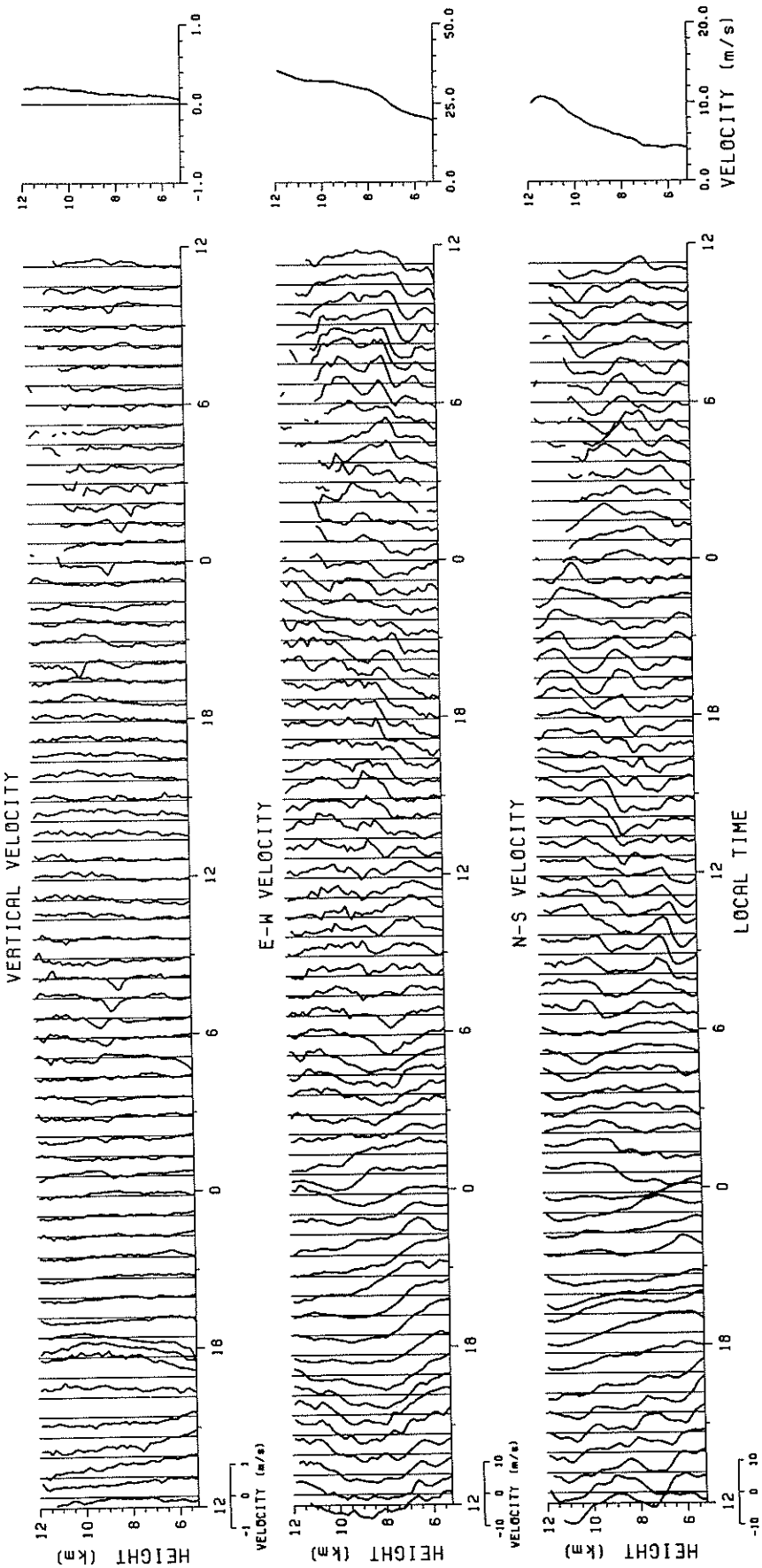

FIG. 6. Height profiles of the fluctuating wind components averaged over approximately 45 min relative to the mean wind averaged over the whole observational period shown on the right-hand side. The upward, eastward and northward velocity components are shown on the top, center and bottom, respectively. The fluctuating velocities are given in reference to the vertical lines at the respective times. The velocity scales are given on the left bottom for each velocity component.

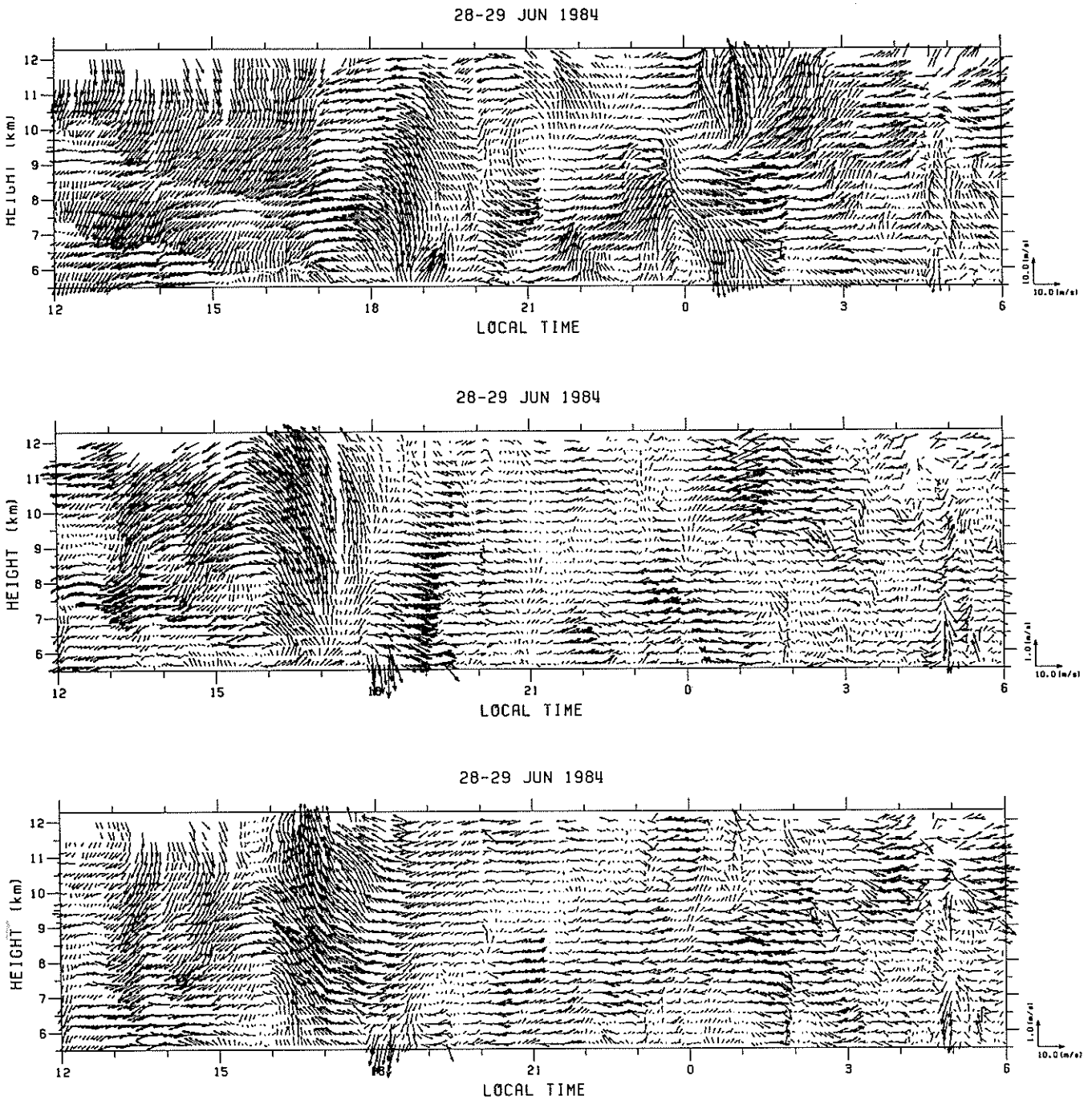

FIG. 7. (a) Horizontal, (b) meridional–vertical and (c) zonal–vertical air flows relative to the mean wind velocities (upward, northward and eastward positive). Time resolution is approximately 5 min. The vertical and horizontal speed scales are indicated in the right bottom.

(iii) those due to a spatial variation moved with a horizontal phase velocity c of structures fixed to the front.

In the present subsection we discuss three features observed in Figs. 5, 6 and 7 mainly from the viewpoints of (ii) and (iii).

First, the precipitation activity (Fig. 5) and low-level jet acceleration (Fig. 6) can be well described by viewpoint (iii), because they seem to be strongly correlated with a mesoscale cyclone as well as a developed cloud system which covered the MU radar site in the evening of 28 June (Fig. 3). This is consistent with various evidence reported by, e.g., Ninomiya and Akiyama (1971)

and Akiyama (1979) that Baiu precipitation is predominantly governed by lower tropospheric conditions. If the cyclone is identified with a frontal fold in Fig. 1 (see the last paragraph of section 4), we may estimate the zonal phase velocity as $c_x \sim 15$ m s$^{-1} \sim 50$ km h^{-1}. However, it should be noted here that the identification of Baiu frontal cyclones, in general, cannot be objectively made, since they are organized by mesoscale and microscale phenomena.

Second, it was shown in Fig. 5 that two intense echo layers descended with a speed on the order of 1 km h^{-1} in the afternoon of 28 June. In view of (iii), if the echo layers were inclined zonally, the inclination would be estimated to be 1 km h$^{-1}/c_x \sim 1/50$. On the other hand, if they were inclined meridionally, a phase speed of $c_y \sim 15$ km h^{-1}, with which the front moved northward in the surface chart (Fig. 3), would lead to an inclination of 1 km h$^{-1}/c_y \sim 1/15$. Next, the mean zonal and meridional velocities near the echo layers are estimated from Fig. 6 as $\bar{u}_x \sim 20$ m s$^{-1} \sim 70$ km h^{-1} and $\bar{u}_y \sim 0$, respectively. Then, in view of (ii), the zonal and meridional inclinations of the echo layers become 1/70 ($\sim$1 km h$^{-1}/\bar{u}_x$) and infinitely large (1 km h$^{-1}/\bar{u}_y$), respectively. Thus, none of these estimations are smaller than the mean frontal inclination (i.e., less than 1/100 meridionally and much smaller zonally; see Fig. 4), and the echo layers are not considered to be fixed to the front or synoptic-scale motions.

While the intense echo layers exist, the horizontal wind, in particular the meridional component, shows a wavelike fluctuation as illustrated in Fig. 6. This seems to be consistent with a general observational feature that intense echoes are associated with strong turbulence which is generated in large wind shear regions. The vertical wavelength of this wavelike fluctuation is about 3 km, which is on the same order as that of inertial–gravity wavelike variations found by Ninomiya (1983) based on rawinsonde observations. Recently, Hirota and Niki (1986) analyzed a similar vertical wavelength near the tropopause jet stream from MU radar data from a winter period. If the echo layers correspond to such an inertial gravity wave, they do not follow the synoptic-scale flows or structures of (ii) or (iii).

Finally, a meridional circulation pattern is observed during the period when the abovementioned echo layers appear. The circulation preceeds the intense updraft of 1630–1800 LST (Fig. 7b). The time scale of this circulation is estimated to be about 5 h. In view of (iii) its zonal and meridional scales are estimated as 250 and 75 km, respectively. In view of (ii) they become 350 and 0 km, respectively. Therefore, if the observed feature is a spatial structure, it is zonally elongated with a horizontal scale of several hundreds of kilometers. Such a scale is intermediate between the so-called mesoα and mesoβ scales, and is much larger than the usual cumulus convection scale and smaller than the mesoscale cyclone scale.

The updrafts in the circulation pattern are not accompanied by surface precipitations (Fig. 5). Generally speaking, the upper-tropospheric wind variations (Figs. 6 and 7) do not seem to be directly related with the cyclone passage. The steady, symmetric structure pointed out in section 4 is formed more perfectly in the upper troposphere. The spatial scale derived above is somewhat larger than that of the cloud clusters found in satellite imageries (e.g., Akiyama, 1984). Based on these considerations neither viewpoint (ii) nor (iii) is expected to uniquely explain the circulation pattern.

In the next subsection, we consider the upper-tropospheric mesoscale wind variations observed by the MU radar mainly in view of (i), although strictly speaking, the circulation pattern should be considered from the four-dimensional viewpoint (in both time and space). The viewpoint of (i) may be acceptable not only because of the dimensional restriction of our observation but also because of some evidence shown below. Throughout the observational period the pseudo-isentropes were relatively sparse between the Baiu front and the tropopause (Fig. 4). They are much denser above the tropopause as is well known, but their intervals near the tropopause were not uniform. These features suggest first that the stratification is less stable even in the upper troposphere, and then that some strong mesoscale convective motions might infiltrate into the stratosphere as pointed out in subsection 6a. Thus, the phenomena could be recognized as those appearing sporadically on a small area in a rather homogeneous region on large scales, so that we may be allowed to base our interpretations on (i) at least at the present quick-look stage of this paper.

c. *Intense updraft events*

It has been pointed out in subsection 5b that the intense updraft events appear at an interval of about 22 h. By the MU radar similar events were observed in no small number during the Baiu and Shurin periods in 1985–86.

Akiyama (1978, 1984) reported on a quasi-diurnal change of cloud cluster, which seemed to be correlated with LST. A 2.5-day period variation was found by Yoshizumi (1978) in upper tropospheric winds, but no shorter period variation has been found in rawinsonde observations. We consider that the observed intense updrafts may not be caused by diurnal differential heating, because they are not correlated with LST.

Further, it is noticed that the 22 h interval is very close to the inertial period $2\pi/f$ (=20.9 h at 34.85°N; f: Coriolis frequency). However, for the observed horizontal winds this periodicity is not predominant, although the inertial oscillation is essentially a horizontal circular motion. So different types of motion should be considered for interpretation of the intense updraft events.

The so-called "conditional symmetric instability" has been discussed as a possible mechanism of meso-

scale rainband formation near a front in the lower troposphere when the Richardson number J in the moist-air sense is less than unity (e.g., Bennets and Hoskins, 1979). The most unstable eigenfrequency ω (imaginary) of the symmetric instability is given by

$$\omega^2 = f^2(1 - 1/J), \tag{1}$$

in the simplest case solved by Stone (1966). However, in the atmosphere observed here,

$$J = \frac{g\dfrac{\partial \ln\theta e}{\partial z}}{\left(\dfrac{\partial u}{\partial z}\right)^2} \sim \frac{10\left(\dfrac{\ln 350 - \ln 340}{6000}\right)}{\left(\dfrac{15}{6000}\right)^2} \sim 8 \tag{2}$$

where the mean vertical gradient of the equivalent potential temperature θe is referred to the JMA rawinsonde data (Fig. 4), while the zonal flow u is referred to the MU radar data (Fig. 6). Thus, as far as such a synoptic-scale situation is concerned, the conditional symmetric instability mechanism cannot work in the observed upper troposphere.

On the other hand, when $J > 1$, there can exist a neutral symmetric motion, and ω of (1) becomes a real frequency. Using the same values as for the above estimation, the period of this motion is $2\pi/\omega = 22$ h. This mode corresponds to a special case of the inertial–gravity waves of zero vertical group velocity that are almost frozen in the altitude range of generation (Yamanaka, 1985). The neutral symmetric motion also has horizontal components but their magnitude may not be so large as to distinguish them from other quasi-horizontal (geostrophic) variations. Although it may be beyond the context of this observational paper to discuss this problem in detail, the coincidence of the observed interval of the updraft events with the frozen-in period of the neutral symmetric motion should be noted.

7. Conclusions

An observation of the Baiu front as a subtropical stationary front has been made with the aid of the MU radar. Three velocity components of air motion are obtained with time and height resolutions of 100 s and 150 m, respectively, which are much superior to those of conventional instruments such as rawinsondes.

Both wind vector and echo power variations observed by the MU radar have been compared with mesoscale meteorological features observed at 12 h intervals by the JMA rawinsondes. Based on this general consistency, the detailed structure of the wind vector pattern and echo intensity has been investigated. A summary of the present work is presented below.

1) The observed mean meridional motion is found to be upward and northward as expected, but deviates upward from the frontal surface and pseudo-isentropes. This seems to be related to active convective clouds on the tropical side of the subtropical front in the upper troposphere.

2) Also, it is observed that upper-tropospheric mesoscale wind variations are not strongly correlated with lower-tropospheric frontal activity such as precipitation. Further studies on the activities of cloud clusters and internal gravity waves are needed to elucidate the mechanism of upper- and lower-troposphere interaction.

3) Particularly noted in the present paper is the intense updraft events with a magnitude of 0.5–1 m s^{-1}. The intense updraft events appear at intervals of about 22 h. From the period of these events and from the fact that no conspicuous change with the same period is found in the horizontal winds, the updraft events are considered to be caused by a neutral symmetric motion that is almost frozen in the altitude range of generation.

Admitting that the single station radar observation cannot distinguish temporal and spatial variations, the VHF Doppler radar such as the MU radar is expected to provide new information on Baiu and other mesometeorological phenomena. Finally, the importance of the MU radar observations is to be noted in the meteorological point of view, since the climatological situation of Japan which is located in the east Asian sector has a lot of interesting phenomena, both tropical and midlatitudinal, as investigated in the present study.

Acknowledgments. The authors wish to thank S. Saito and H. Tanaka of Nagoya University, I. Takayabu of Tokyo University, and an anonymous reviewer of the present paper for interesting suggestions and constructive comments. Thanks are also due to W. L. Oliver, Jr. and P. T. May of the Radio Atmospheric Science Center, Kyoto University, for their careful reading of the manuscript. They are indebted also to T. Abe of the Department of Electrical Engineering, Kyoto University, for his assistance in the data analysis. The work of one of the authors (M.D.Y.) was supported by the Japan Society for the Promotion of Science (JSPS) under the Fellowships for Japanese Junior Scientists, and partially by the Grant-in-Aid of the Ministry of Education, Science and Culture of Japan. The MU radar belongs to and is operated by the Radio Atmospheric Science Center of Kyoto University.

REFERENCES

Akiyama, T., 1978: Mesoscale pulsation of convective rain in medium-scale disturbances developed in Baiu front. *J. Meteor. Soc. Japan,* **56,** 267–283.

——, 1979: Thermal stratification in Baiu frontal medium-scale disturbances with heavy rainfalls. *J. Meteor. Soc. Japan,* **57,** 587–598.

——, 1984: A medium-scale cloud cluster in a Baiu front. Part I: Evolution process and fine structure. *J. Meteor. Soc. Japan,* **62,** 485–504.

Balsley, B. B., and K. S. Gage, 1980: The MST radar technique:

Potential for middle atmospheric studies. *Pure Appl. Geophys.*, **118,** 452–493.

——, and ——, 1982: On the use of radars for operational wind profiling. *Bull. Amer. Meteor. Soc.*, **63,** 1009–1018.

Bennets, D. A., and B. J. Hoskins, 1979: Conditional symmetric instability: A possible explanation for rainbands. *Quart. J. Roy. Meteor. Soc.*, **105,** 945–962.

Ecklund, W. L., K. S. Gage, B. B. Balsley, R. G. Strauch and J. L. Green, 1982: Vertical wind variability observed by VHF radar in the lee of the Colorado Rockies. *Mon. Wea. Rev.*, **110,** 1451–1457.

——, B. B. Balsley, D. A. Carter, A. C. Riddle, M. Crochet and R. Garello, 1985: Observations of vertical motions in the closely spaced ST radars. *Radio Sci.*, **20,** 1196–1206.

Fukao, S., S. Kato, T. Aso, M. Sasada and T. Makihira, 1980: Middle and upper atmosphere radar (MUR) under design in Japan. *Radio Sci.*, **15,** 225–231.

——, T. Sato, T. Tsuda, M. Yamamoto and S. Kato, 1986: High resolution turbulence observations in the middle and lower atmosphere by the MU radar with fast beam steerability: preliminary results. *J. Atmos. Terr. Phys.*, **48,** 1269–1278.

——, ——, ——, S. Kato, K. Wakasugi and T. Makihira, 1985a: The MU radar with an active phased array system, 1. Antenna and power amplifiers. *Radio Sci.*, **20,** 1155–1168.

——, T. Tsuda, T. Sato, S. Kato, K. Wakasugi and T. Makihira, 1985b: The MU radar with an active phased array system, 2. In-house equipment. *Radio Sci.*, **20,** 1169–1176.

——, K. Wakasugi, T. Sato, S. Morimoto, T. Tsuda, I. Hirota, I. Kimura and S. Kato, 1985c: Direct measurement of air and precipitation particle motion by VHF Doppler radar. *Nature*, **316,** 712–714.

——, ——, ——, T. Tsuda, I. Kimura, N. Takeuchi, M. Matsuo and S. Kato, 1985d: Simultaneous observation of precipitating atmosphere by VHF band and C/Ku band radars. *Radio Sci.*, **20,** 622–630.

Gage, K. S., and B. B. Balsley, 1984: MST radar studies of wind and turbulence in the middle atmosphere. *J. Atmos. Terr. Phys.*, **46,** 739–753.

Green, J. L., K. S. Gage and T. E. VanZandt, 1979: Atmospheric measurements by VHF pulsed Doppler radar. *IEEE Trans. Geosci. Electron.*, **GE-17,** 262–280.

Gossard, E. E., 1979: A fresh look at the radar reflectivity of clouds. *Radio Sci.*, **14,** 1089–1097.

Harper, R. M., and W. E. Gordon, 1980: A review of radar studies of the middle atmosphere. *Radio Sci.*, **15,** 195–211.

Hirota, I., and T. Niki, 1986: Inertia-gravity waves in the troposphere and stratosphere observed by the MU radar. *J. Meteor. Soc. Japan*, **64,** 995–999.

Hobbs, P. V., 1978: Organization and structure of clouds and precipitation on the mesoscale and microscale in cyclonic storms. *Rev. Geophys. Space Phys.*, **16,** 741–755.

Holton, J. R., 1984: Troposphere-stratosphere exchange of trace constituents: The water vapor pazzle. *Dynamics of the Middle Atmosphere*, J. R. Holton and T. Matsuno, Eds. pp. 369–385, Terra, Tokyo.

Japan Meteorological Agency, 1984a: *Daily Weather Maps and Data*, June 1984. 240 pp.

——, 1984b: *Monthly Report of Meteorological Satellite Center*, June 1984. 263 pp.

——, 1984c: *Aerological Data of Japan*, June 1984. 239 pp.

Kato, S., T. Ogawa, T. Tsuda, T. Sato, I. Kimura and S. Fukao, 1984: The middle and upper atmosphere radar: First results using a partial system. *Radio Sci.*, **19,** 1475–1484.

——, T. Tsuda, M. Yamamoto, T. Sato and S. Fukao, 1986: First results observed by the MU radar in full operation. *J. Atmos. Terr. Phys.*, **48,** 1259–1267.

Larsen, M. F., and J. Röttger, 1982: VHF and UHF Doppler radars as tools for synoptic research. *Bull. Amer. Meteor. Soc.*, **63,** 996–1008.

Matsumoto, S., S. Yoshizumi and M. Takeuchi, 1970: On the structure of the Baiu front and the associated intermediate-scale disturbances in the lower atmosphere. *J. Meteor. Soc. Japan*, **48,** 479–491.

Murakami, T., 1951: On the study of the change of the upper westerlies in the last stage of Bai-u season (rainy season in Japan). *J. Meteor. Soc. Japan*, **29,** 162–175, (in Japanese.)

Ninomiya, K., 1983: Internal-gravity-wave-like variations of temperature, humidity and wind observed in the troposphere downstream of heavy rainfall area. *J. Meteor. Soc. Japan*, **61,** 163–169.

——, 1984: Characteristics of Baiu front as a predominant subtropical front in the summer northern hemisphere. *J. Meteor. Soc. Japan*, **62,** 880–894.

——, and T. Akiyama, 1971: The development of the medium-scale disturbance in the Baiu front. *J. Meteor. Soc. Japan*, **49,** 663–677.

——, and ——, 1972: Medium-scale echo clusters in the Baiu front as revealed by multi-radar composite echo maps. Part I. *J. Meteor. Soc. Japan*, **50,** 558–569.

——, M. Ikawa and T. Akiyama, 1981: Long-lived medium-scale cumulonimbus cluster in Asian subtropical humid region. *J. Meteor. Soc. Japan*, **59,** 564–577.

Röttger, J., 1979: VHF radar observations of a frontal passage. *J. Appl. Meteor.*, **18,** 85–91.

——, 1984: The MST radar technique. *Handbook for MAP*, Vol. 13, R. A. Vincent, Ed., pp. 187–232, University of Illinois, Urbana, Ill.

——, and G. Schmidt, 1981: Characteristics of frontal zones determined from spaced antenna VHF radar observations. *Proc. 20th Conf. on Radar Meteorology*, Boston, Amer. Meteor. Soc., 30–37.

Shapiro, M. A., 1980: Turbulent mixing within tropopause folds as a mechanism for the exchange of chemical constituents between the stratosphere and troposphere. *J. Atmos. Sci.*, **37,** 994–1004.

Stone, P. H., 1966: On non-geostrophic baroclinic stability. *J. Atmos. Sci.*, **23,** 390–400.

Tsuda, T., M. Yamamoto, T. Sato, S. Kato and S. Fukao, 1985: Comparison observations between the MU radar and the Kyoto meteor radar. *Radio Sci.*, **20,** 1241–1246.

Tokioka, T., 1973: A stability study of medium-scale disturbances with inclusion of convective effects. *J. Meteor. Soc. Japan*, **51,** 1–10.

Wakasugi, K., S. Fukao, S. Kato, A, Mizutani and M. Matsuo, 1985: Air and precipitation particle motions within a cold front measured by the MU VHF radar. *Radio Sci.*, **20,** 1233–1240.

——, A. Mizutani, M. Matsuo, S. Fukao and S. Kato, 1986: A direct method for deriving drop-size distribution and vertical air velocities from VHF Doppler radar spectra. *J. Atmos. Oceanic Technol.*, **3,** 623–629.

Yamanaka, M. D., 1985: Inertial oscillation and symmetric motion induced in an inertio-gravity wave critical layer. *J. Meteor. Soc. Japan*, **63,** 715–737.

Yoshino, M. M., 1977: Bai-u, the rainy season in early summer. *The Climate of Japan*, E. Fukui, Ed., pp. 85–101, Kodansha/Elsevier, Tokyo.

Yoshizumi, S., 1978: On an upper tropospheric disturbance of 2.5-day period around the jet stream in the Baiu frontal zone. *J. Meteor. Soc. Japan*, **56,** 243–252.